Aquaculture 584 (2024) 740680

Contents lists available at ScienceDirect

Aquaculture

journal homepage: www.elsevier.com/locate/aquaculture

Determining patterns of tissue tropism for IHHNV, GAV and YHV-7 infection in giant black tiger shrimp (*Penaeus monodon*) using real-time RT-qPCR

P.M. Arbon [a,b,*], M. Andrade Martinez [a,b], M. Garrett [a,b], D.R. Jerry [a,b,c,d], K. Condon [a,b,d]

[a] JCU AquaPATH Detection Laboratory, James Cook University, Townsville 4814, Queensland, Australia
[b] Centre for Sustainable Tropical Fisheries and Aquaculture, James Cook University, Townsville 4814, Queensland, Australia
[c] Tropical Futures Institute, James Cook University, Singapore
[d] ARC Research Hub for Supercharging Tropical Aquaculture through Genetic Solutions, James Cook University, Townsville 4814, Queensland, Australia

ARTICLE INFO

Keywords:
Aquaculture
Pathogen detection
TaqMan
Viral distribution
Sampling

ABSTRACT

Disease management in shrimp aquaculture is heavily dependent on accurate and rapid pathogen detection and diagnosis. Understanding the presence and distribution of pathogens within various tissues of the shrimp host is critical to ensure detection efforts are targeted for optimal sensitivity and reliability. Modern advancements in molecular technologies, including nucleic acid extraction and RT-qPCR, have yielded significant improvements in pathogen detection capabilities. Despite these advancements and their widespread adoption within both research and industry applications, evidence to inform their optimised use, such as revisions to tissue-specific viral detection to support selection of appropriate target tissues, has not been established. To address these gaps, this study aimed to establish contemporary evidence of viral tissue tropism for three major shrimp pathogens. TaqMan qPCR analysis was used to determine tissue-specific loading of viral pathogens in naturally infected *Penaeus monodon* pleopod, gill, hepatopancreas, lymphoid organ, abdominal muscle tissue, hindgut and ventral nerve cord. The viral targets analysed included *Penaeus stylirostris penstyldensovirus* 1 (PstDV1), formerly named infectious hypodermal haematopoietic necrosis virus (IHHNV) and, two genotypes of the yellow head virus complex, including genotype 2 known as gill associated virus (YHV-2/ GAV), and genotype 7 (YHV-7). QPCR analyses demonstrated the highest level of genetic IHHNV detection from gill tissue, followed sequentially by hindgut, pleopod, hepatopancreas, lymphoid organ, ventral nerve cord and abdominal muscle. For the yellow head viruses (GAV and YHV-7), no significant differences in genetic viral detection were demonstrated, although a non-significant advantage was observed for lymphoid organ and hindgut tissue. Beyond establishing contemporary evidence of viral distribution to improve understanding of host-viral interactions, these findings offer supporting evidence for revisions to appropriate target tissue recommendations, within the World Organisation for Animal Health (WOAH, founded as OIE) Manual of Diagnostic Tests for Aquatic Animals, for optimised modern shrimp pathogen detection.

1. Introduction

Rapid expansion and intensification of global aquaculture has coincided with the rise of aquatic diseases (Kennedy et al., 2016; Pulkkinen et al., 2010; Walker and Winton, 2010). Consequently, effective disease management presents a central challenge for both sustaining current, and increasing future aquaculture production (Stentiford et al., 2017; Stentiford et al., 2012). Reliable and rapid pathogen detection and disease diagnosis is fundamental to effective disease management in aquaculture (Kumar et al., 2022; Lightner and Redman, 1998; WOAH, 2023).

While diseases are of major concern across the diversity of primary aquaculture species, shrimp aquaculture is one of the most severely impacted (Asche et al., 2021; Leung and Bates, 2013). Global shrimp production endures sustained impacts from diseases that range from reduced productivity via disorders of fecundity and growth, to outbreaks of diseases resulting in mass mortality events (Shinn et al., 2018; Valappil et al., 2021). Currently, shrimp pathogen detection for

* Corresponding author at: Aquaculture Department, James Cook University, Douglas, QLD 4811, Australia.
E-mail address: phoebe.arbon@jcu.edu.au (P.M. Arbon).

https://doi.org/10.1016/j.aquaculture.2024.740680
Received 24 October 2023; Received in revised form 15 January 2024; Accepted 15 February 2024
Available online 16 February 2024

surveillance and diagnostics relies primarily on real-time quantitative PCR (qPCR) analysis due to its availability, utility, diagnostic specificity, sensitivity, and scalability of throughput (WOAH, 2023).

Application of technologies, including PCR and qPCR, for the detection and diagnosis of aquatic diseases is guided by the World Organisation for Animal Health (WOAH, founded as OIE). The WOAH Manual of Diagnostic Tests for Aquatic Animals (herein referred to as the Aquatic Manual), provides information to support a standardised and validated approach for the detection and diagnosis of diseases listed in the WOAH Aquatic Animal Health Code (herein referred to as the Aquatic Code) (WOAH.org). Since the first edition in 1995, successive editions of the Aquatic Code and Aquatic Manual have expanded in response to the emergence of new pathogens and improved diagnostic technologies. Expansions have incorporated new chapters and updates to recommended practices in line with the latest developments in knowledge. However, some sections have evolved more rapidly, outpacing revisions to supporting sections. For example, where the definition of suitable target tissues for diagnosis and surveillance has remained unchanged, despite the significantly improved detection sensitivity and reliability of the updated detection practices. Definition and recommendation of appropriate target tissues is crucial to support sensitive pathogen detection and efficient sampling practices. Inconsistent updates to these sections may result in the sampling and analysis of suboptimal tissue types, resulting in a loss of efficiency and detection accuracy (Hou et al., 2023). Conversely, the non-inclusion of tissue types that may be suitable for detection of a broad range of pathogen targets may result in multiple tissue analysis that needlessly increases costs of surveillance.

Accordingly, this study aimed to generate evidence supporting appropriate target tissue selection for viral pathogen detection using contemporary techniques. Our study investigated tissue-specific qPCR detection of *Penaeus stylirostris penstyldensovirus* 1 (PstDV1) (ICTV, 2023), formerly named and herein referred to as infectious hypodermal haematopoietic necrosis virus (IHHNV) and, two genotypes of the yellow head virus complex, including genotype 2 known as gill associated virus (YHV-2, GAV), and genotype 7 (YHV-7), in naturally infected giant black tiger shrimp, *Penaeus monodon.*

2. Material and methods

2.1. Experimental animals

Two cohorts of shrimp were used for analysis in this study. Cohort 1 ($n = 10$, 35.99 ± 6.63 g) originated from a commercial shrimp farm in Queensland, Australia and were known to be naturally infected with both IHHNV and GAV based on previous qPCR and reverse transcriptase (RT) qPCR pathogen screening conducted throughout the production cycle. Cohort 2 ($n = 10$, 37.46 ± 9.17 g) originated from a commercial shrimp farm in Queensland, Australia and were known to be naturally infected with YHV-7 based on previous RT-qPCR pathogen screening conducted throughout the production cycle.

2.2. Sample collection

Seven tissues including pleopod (PLEO), gill (GILL), hepatopancreas (HP), lymphoid organ (LO), hindgut (HG), ventral nerve cord (NER) and, abdominal tail muscle (TAIL), were sampled from each individual shrimp (Fig. 1). Each tissue sample was weighed and placed immediately into 2 mL Lysing Matrix D tubes (MP Biomedicals™) containing 350 μL of MagMAX™ CORE Lysis Solution (Applied Biosystems™). Samples were stored at ambient temperature (~25 °C) in lysis solution for 48 h prior to nucleic acid extraction.

2.3. Nucleic acid extraction

Nucleic acid extraction was conducted as per Arbon et al. (2022) with minor adaptaion. Briefly, 5 μL of 20 mg ml^{-1} MagMAX™ CORE Proteinase K (Applied Biosystems™) was added to each 2 mL Lysing Matrix D tube (MP Biomedicals™) containing the sample and 350 μL of MagMAX™ CORE Lysis Solution (Applied Biosystems™). Samples were homogenised for 30 s at 5000 rpm and incubated at ~72 °C for 60 min. Total nucleic acid (TNA) extraction was conducted using the MagMAX™ CORE Nucleic Acid Purification Kit (Applied Biosystems™) with a KingFisher™ Flex 96 Deep-Well Magnetic Particle Processor (ThermoFisher Scientific™) as per the manufacturer's instructions. All tissue samples belonging to each experimental cohort were extracted on 96 well plates together using the same reagent batches to minimise inter-run variation on nucleic acid extraction. TNA was eluted into 100 μL of MagMAX™ CORE Elution Buffer (Applied Biosystems™). Template was stored at −20 °C until required.

2.4. Quantitative real-time PCR (qPCR)

RT-qPCR and qPCR analysis was used for the detection of GAV and IHHNV from cohort 1, and YHV-7 from cohort 2. Additionally, the *Penaeus monodon* Dicer-1 gene (Dicer-1) (Su et al., 2008) was targeted for detection using RT-qPCR as a protocol integrity control (Table 1). Target DNA and RNA in each TNA extract were quantified using TaqMan Real-Time quantitative PCR (qPCR). For the detection of IHHNV (DNA target), the SensiFAST™ Probe Lo-ROX Kit (Meridian Bioscience™) was used. For the detection of GAV (YHV-2), YHV-7 and Dicer-1 (RNA targets), the reverse transcriptase (RT) SensiFAST™ Probe Lo-ROX One-Step Kit (Meridian Bioscience™) was used. A total of 1.25 μL of sample template was added to 8.75 μL of master-mix to yield a 10 μL reaction;

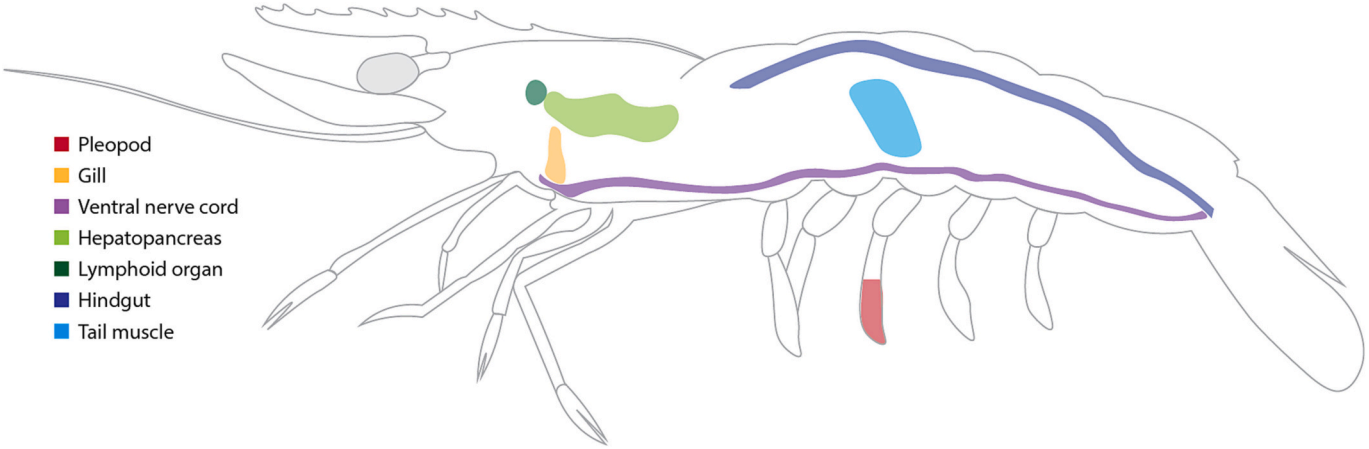

Fig. 1. Tissue specific sample collection diagram.

Table 1
Quantitative polymerase chain reaction (qPCR) primer and probe details, as used in the present study.

Genetic target	Primer/ Probe	Sequence [5′-3′]	Product length [bp]	Reference
IHHNV	IHHNV 309 qF	CCTAAAGAAAACAGTGCAGAATAT	98	(Cowley et al., 2018)
	IHHNV 309 qR	TCATCGTCAAGTTTATTGACAAGTTC		
	IHHNV 309 qProbe	CTCCAACACTTAGTCAAA		
YHV-2 *syn* GAV	GAV-qF	GGGATCCTAACATCGTCAACGT	81	(De La Vega et al., 2004)
	GAV-qR	AGTATGGATTACCCTGGTGCAT		
	GAV-qProbe	TCAGCCGCTTCCGCTTCCAATG		
YHV-7	YHV7-qF	CATCCAACCTATCGCCTACA	79	(Cowley et al., 2019)
	YHV7-qR	TGTGAAGTCCATGTGAACGA		
	YHV-7 qProbe	CAACGACAGACACCTCATCCGTGA		
Dicer-1	Dicer-1 qF	TGGTACCAAAGTCACCCATTAG	91	(Su et al., 2008)
	Dicer-1 qR	ACCTTCCCATCAACAAGACGTT		
	Dicer-1 qProbe	AACCAGAAACAGCCAAAT		

inclusive of 0.1 μL of the respective target primers (0.2 μM final concentration) and 0.025 μL of target probe (0.05 μM final concentration). Primer and probe sequences are listed in Table 1. Analysis was conducted using a QuantStudio™ 5 Real-Time PCR System, 384-well (Applied Biosystems™). Cycle conditions were standardised for both DNA and RNA targeting assays, consisting of a reverse-transcription (RT) step of 45 °C for 10 min, initial denaturation at 95 °C for 5 min, followed by 45 cycles of denaturation at 95 °C for 10 s and annealing and extension at 60 °C for 30 s. Raw data were processed using QuantStudio™ Design & Analysis Software v1.5.2 (ThermoFisher Scientific™), using the ΔRn method with a relative threshold of 0.05, to produce cycle threshold (Ct) values of positive detections. Samples which did not amplify beyond the relative threshold within 45 cycles were categorised as undetected.

To minimise non-biological variation introduced during qPCR analysis, three 1.25 μL aliquots of each TNA extract were tested as technical replicates for each target. Technical replicates of TNA extracts that were extracted on the same 96-well plate were tested on the same 384-well plate using the same reagent batches to minimise inter-run variation. Within each analysis run, a non-template control and positive nucleic acid control for each target were included in triplicate.

Serial 10-fold dilutions of gBlock™ Gene Fragments (Integrated DNA Technologies™, NSW, Australia) were used as synthetic linear dsDNA template for IHHNV, GAV and YHV-7. The gBlock™ Gene Fragments were designed to comprise the genomic sequence of each pathogen targeted by the qPCR or RT-qPCR assays described in Table 1, including flanking sequence, derived from sequences available on the National Centre for Biotechnology Information (NCBI) database. Each point on the 10-fold dilution series was analysed in triplicate by qPCR. Each dilution series were used to generate standard curves, from which the conversion of Ct value to target copy number (μL^{-1}) could be estimated. Calculated target copy number μL^{-1} TNA extract was standardised to target copy number mg^{-1} tissue for each sample for further analyses. Samples categorised as undetected were assumed to have a viral copy number mg^{-1} tissue of zero.

2.5. Statistical analysis

Statistical analysis was conducted using R (R Core Team, 2022). Descriptive statistical parameters were calculated for each target and between tissue types. For individual shrimp, tissues were ranked from 1 to 7, with a rank of 1 representing the tissue yielding the highest copy number mg $^{-1}$ for that specific shrimp, and 7 representing the lowest. The mean and modal rank of each tissue type was calculated for shrimp within each cohort, for each pathogen target. Further statistical analysis to evaluate the differences in copy number and correlation of detection between tissues were conducted using $\log_{10}$ transformed copy number mg^{-1} tissue, after zero values were adjusted to one. Significant differences in IHHNV and YHV-7 detection between the various tissue types were determined using an ANOVA with Tukey HSD post-hoc test. Differences in GAV detections were determined using Kruskal-Wallis analysis with Dunn test post-hoc analysis (Ogle et al., 2022) due to significant deviation from homogeneous variances, as determined via a Levene's test (Fox and Weisberg, 2019). The statistical relationship of target detections between the various tissue types for individual shrimp was determined using Pearson's correlation analysis (Harrell, 2023).

3. Results

3.1. Overall detection of pathogens

Detection of IHHNV across all tissue types ranged between 1.2×10^4 and 1.58×10^8 copies mg^{-1} tissue, yielding the highest average copy number of the three targets analysed (mean ± SD; $2.2 \times 10^7 \pm 3.15 \times 10^7$ copies mg^{-1} tissue). YHV-7 detection across all tissue types ranged between 1.3 and 9.66×10^6 copies mg^{-1} tissue, yielding an average detected copy number of $4.6 \times 10^5 \pm 1.49 \times 10^6$ copies mg^{-1} tissue (mean ± SD). GAV was detected at the lowest average copy number across all tissue types of the three viral targets analysed. GAV detections ranged from no detection to 3.52×10^6 copies mg^{-1} tissue (mean ± SD; $7.4 \times 10^4 \pm 4.28 \times 10^5$ copies mg^{-1} tissue). Tissue-specific detection levels for the shrimp analysed in this study are detailed in Table 2.

3.2. IHHNV

Detection of IHHNV was the highest and most consistent across tissue types for all pathogen targets analysed, ranging between $\sim 10^4$ and 10^8 copies mg^{-1} tissue (Table 2), with a maximum $\log_{10}$ fold difference in copies mg^{-1} tissue of 1.5 between tissues of the same shrimp (TAIL: 5.06×10^6, LO: 1.53×10^8). Overall, per mg of tissue, average IHHNV copy number was highest in GILL, followed sequentially by HG, LO, PLEO, HP, NER, and TAIL (Fig. 2A). Mean $\log_{10}$ IHHNV copy number mg^{-1} tissue varied significantly between tissue types ($f_6 = 4.39$, $p = 0.000915$). On average, GILL yielded significantly higher detection of IHHNV than both NER ($p = 0.013$) and TAIL ($p = 0.003$). HG yielded significantly higher detection than TAIL ($p = 0.022$). When tissues were ranked to represent highest to lowest copy number detected within individual shrimp, on average, GILL ranked as the best tissue, followed by HG, PLEO, HP, LO, NER and TAIL. Analysing tissue ranking for individual shrimp, as opposed to observing the average IHHNV copy number for each tissue across the whole cohort, HP and PLEO were revealed to be more consistently advantageous for the detection of IHHNV than LO, despite yielding lower average copy number across the cohort. IHHNV copy number mg^{-1} were significantly linearly correlated between all tissue types within individual shrimp ($r \geq 0.65$, $p \leq 0.05$; Fig. 2B).

3.3. GAV

Detected GAV was lower than the detected IHHNV copies mg^{-1} tissue from cohort 1 (GAV mean copy number mg^{-1} tissue $\sim 10^4$; Table 2).

Table 2
IHHNV, GAV and YHV-7 detection in different tissues of naturally infected *Penaeus monodon* (GILL = gill, HG = hindgut, HP = hepatopancreas, LO = lymphoid organ, NER = ventral nerve cord, PLEO = pleopod, TAIL = tail muscle). Tissue quantity (mg) used in TNA extraction for each shrimp is given as mean ± SD for each tissue type. Mean and modal tissue rank (1 = highest detection to 7 = lowest detection) from individual shrimp was calculated for each pathogen across all shrimp, within each relevant cohort (IHHNV and GAV in cohort 1, YHV-7 in cohort 2).

Tissue		IHHNV copy mg^{-1} tissue			GAV copy mg^{-1} tissue			YHV-7 copy mg^{-1} tissue		
Type	Weight (mg) mean ± SD	Rank mean (mode)	Mean ± SD	Min - max	Rank mean (mode)	Mean ± SD	Min - max	Rank mean (mode)	Mean ± SD	Min - max
GILL	40.76 ± 15.82	1.6 (1)	$5.0 \times 10^7 \pm 4.15 \times 10^7$	1.4×10^6–1.05×10^8	4.2 (6)	$2.3 \times 10^2 \pm 3.49 \times 10^2$	1.8×10^1–1.17×10^3	3.8 (3)	$1.3 \times 10^5 \pm 1.98 \times 10^5$	3.3×10^1–6.35×10^5
HG	90.13 ± 33.88	2.5 (2)	$2.9 \times 10^7 \pm 2.52 \times 10^7$	1.9×10^5–6.79×10^7	2 (2)	$7.6 \times 10^4 \pm 1.15 \times 10^5$	9.2×10^0–3.32×10^5	2.1 (2)	$3.3 \times 10^5 \pm 4.45 \times 10^5$	1.2×10^1–1.44×10^6
HP	144.62 ± 58.31	3.6 (4)	$2.1 \times 10^7 \pm 1.81 \times 10^7$	3.5×10^5–4.66×10^7	4.1 (5)	$2.5 \times 10^3 \pm 4.33 \times 10^3$	6.7×10^{-1} - 1.09×10^4	4.8 (5)	$3.1 \times 10^4 \pm 3.28 \times 10^4$	1.5×10^0–9.90×10^4
LO	23.75 ± 10.24	4 (5)	$2.4 \times 10^7 \pm 4.80 \times 10^7$	1.7×10^5–1.58×10^8	2.2 (1)	$4.4 \times 10^5 \pm 1.10 \times 10^6$	undetected - 3.52×10^6	1.8 (1)	$2.6 \times 10^6 \pm 3.27 \times 10^6$	9.4×10^0–9.66×10^6
NER	80.47 ± 15.78	6.2 (6)	$5.2 \times 10^6 \pm 6.92 \times 10^6$	1.2×10^4–2.09×10^7	5.6 (7)	$2.2 \times 10^2 \pm 3.64 \times 10^2$	undetected - 1.15×10^3	6.6 (7)	$5.8 \times 10^3 \pm 8.66 \times 10^3$	1.3×10^0–2.74×10^4
PLEO	41.93 ± 15.93	3.5 (4)	$2.2 \times 10^7 \pm 2.96 \times 10^7$	6.8×10^5–8.95×10^7	4.9 (7)	$8.9 \times 10^1 \pm 1.13 \times 10^2$	6.4×10^0–3.83×10^2	3.8 (4)	$8.8 \times 10^4 \pm 1.04 \times 10^5$	3.0×10^1–2.42×10^5
TAIL	9.36 ± 4.54	6.6 (7)	$2.1 \times 10^6 \pm 2.01 \times 10^6$	1.4×10^4–5.06×10^6	4.6 (5)	$4.6 \times 10^2 \pm 7.77 \times 10^2$	undetected - 2.56×10^3	5.1 (6)	$1.2 \times 10^4 \pm 1.05 \times 10^4$	3.2×10^1–2.52×10^4

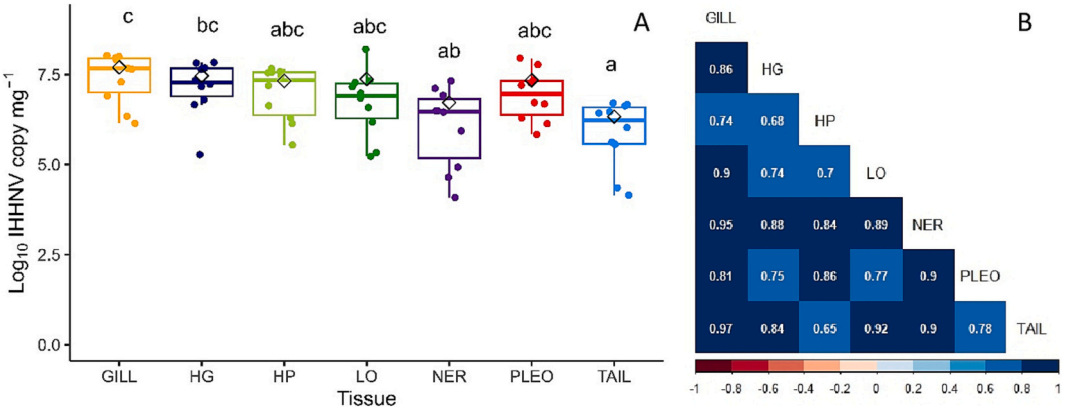

Fig. 2. (A) IHHNV detection in different tissues of naturally infected *Penaeus monodon.* Each point represents the $\log_{10}$(IHHNV copy number mg^{-1} tissue) calculated from the average cycle threshold value of technical triplicate RT-qPCR. Mean $\log_{10}$(IHHNV copy number mg^{-1} tissue) for each tissue are indicated by a black diamond. Letters indicate significant difference between means ($\alpha = 0.05$). (B) Pearson's correlation coefficient matrix of $\log_{10}$(IHHNV copy number mg^{-1} tissue) between tissue types. (GILL = gill, HG = hindgut, HP = hepatopancreas, LO = lymphoid organ, NER = ventral nerve cord, PLEO = pleopod, TAIL = tail muscle).

Detection across tissue types was also less consistent for GAV, ranging from undetected to 10^6 copies mg^{-1} tissue, with a maximum $\log_{10}$ fold difference of 4.4 between tissues of the same shrimp (HP: 1.33×10^2, LO 3.52×10^6). Per mg of tissue, average GAV copy number was highest in LO, followed sequentially by HG, HP, TAIL, GILL, NER and PLEO (Fig. 3A). Despite the apparent inconsistency of GAV detection levels between tissue types, mean $\log_{10}$ GAV copy mg^{-1} tissue did not significantly vary. When tissues were ranked to represent highest to lowest copy number detected within individual shrimp, on average, HG ranked as the best tissue, followed by LO, HP, GILL, TAIL, PLEO and NER. Analysing tissue ranking for individual shrimp compared to observing the average GAV copy number for each tissue across the cohort, HG was revealed to be more consistently advantageous for the detection of GAV than LO. This is likely strongly influenced by the single shrimp from which GAV was undetected in the LO. Similarly, while the cohort averaged GAV copy number detected from TAIL was higher than detection from GILL, ranking tissues in individual shrimp revealed GILL to be more consistently advantageous, likely due to the two shrimp from which GAV was undetected in TAIL. With the same rationale, PLEO ranked better than NER, despite having lower average copy number across the cohort. Except for PLEO and GILL, detection levels in the various tissues of the experimental shrimp were significantly linearly correlated all other tissue types ($r \geq 0.70$, $p \leq 0.05$; Fig. 3B). While copy number mg^{-1} tissue in PLEO and GILL correlated significantly with one another ($r = 0.66$, $p = 0.04$), GAV load in PLEO did not correlate significantly with any other tissue types. Detection in GILL significantly correlated with tissues excluding HG ($r = 0.29$) and HP ($r = 0.47$).

3.4. YHV-7

Detection of YHV-7 across tissue types ranged between <10 and 10^6 copies mg^{-1} tissue (Table 2), with a maximum $\log_{10}$ fold difference of 2.6 between tissues of the same shrimp (GILL: 2.13×10^4, LO: 9.66×10^6). Per mg of tissue, average YHV-7 copy number was highest in LO,

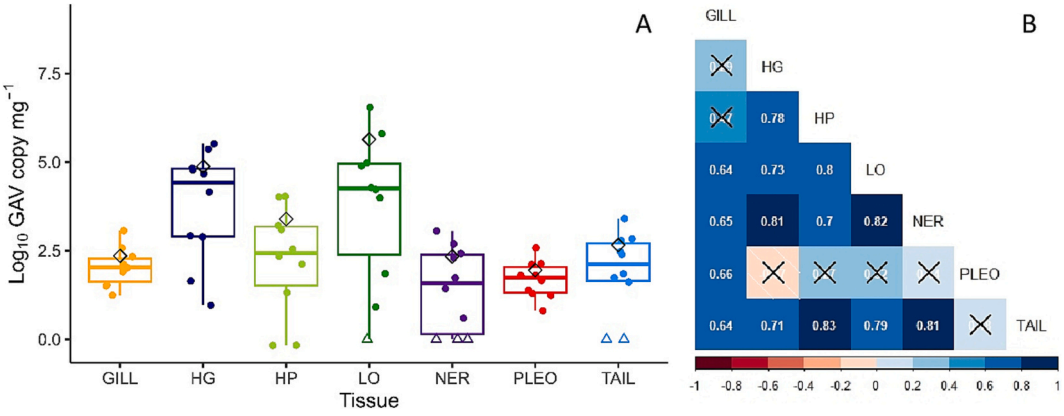

Fig. 3. (A) GAV detection in different tissues of naturally infected *Penaeus monodon*. Each point represents the $\log_{10}$(GAV copy number mg^{-1} tissue) calculated from the average cycle threshold value of technical triplicate RT-qPCR. Tissue samples where GAV was undetected (assigned zero value copy number) are indicated by a triangle. Mean $\log_{10}$(GAV copy number mg^{-1} tissue) for each tissue are indicated by a black diamond. No significant difference between means ($\alpha = 0.05$) were found. (B) Pearson's correlation coefficient matrix of $\log_{10}$(GAV copy number mg^{-1} tissue) between tissue types. Non-significant correlations ($\alpha = 0.05$) are marked by a cross. (GILL = gill, HG = hindgut, HP = hepatopancreas, LO = lymphoid organ, NER = ventral nerve cord, PLEO = pleopod, TAIL = tail muscle).

followed sequentially by HG, GILL, PLEO, HP, TAIL and NER (Fig. 4A). No significant differences were observed for mean $\log_{10}$ YHV-7 copy number mg^{-1} tissue between tissue types. When tissues were ranked to represent highest to lowest copy number detected within individual shrimp, rankings reflected the order of tissues defined by the cohort average YHV-7 copy number mg^{-1} tissue. YHV-7 detection between all tissue types were highly significantly correlated ($r \geq 0.86$, $p \leq 0.001$; Fig. 4B).

3.5. Dicer-1

Dicer-1 was detected consistently from all tissues analysed. No negative correlations between the quantity of tissue used for TNA extraction and the level of Dicer-1 detected were observed within any of the tissue types analysed, suggesting that there was no significant inhibition of DNA extraction or PCR from co-precipitated specimen matrix inhibitors.

4. Discussion

This study aimed to generate contemporary evidence of viral distribution patterns of IHHNV, GAV and YHV-7 using qPCR detection, in naturally infected *P. monodon*. The findings of this study provide modern understanding of infection patterns to improve detection for surveillance and disease diagnosis purposes. This work will also be valuable to support ongoing maintenance and modernisation of the Aquatic Manual, in alignment with the 2021 WOAH Strategy on Aquatic Animal Health.

4.1. IHHNV

IHHNV was listed in the first edition of the Aquatic Code and is the only WOAH listed pathogen that is frequently detected in the Australian shrimp aquaculture industry (Arbon et al., 2022; OIE, 1995; WOAH, 2023). IHHNV is generally described as a systemic virus, infecting tissues of ectodermal and mesodermal origin, and as such, does not replicate in endodermal or enteric tissues. Accordingly, the Aquatic Manual specifically defines hepatopancreas and midgut tissues as unsuitable for surveillance and diagnosis of IHHNV (WOAH, 2023). The historical studies cited to support this exclusion assert that such tissues (endoderm-derived hepatopancreas, midgut and midgut caeca) show no histological signs of infection with IHHNV and are usually negative by in-situ hybridisation (ISH) (Lightner, 1993; Lightner et al., 2009; Lightner et al., 1983; Lightner and Redman, 1998; OIE, 2019; WOAH, 2023). Histology is often used to detect IHHNV-specific Cowdry type A inclusion bodies, which are considered pathognomonic for IHHNV infection. However, recent studies have since confirmed that tissues naturally and experimentally infected with IHHNV frequently lack

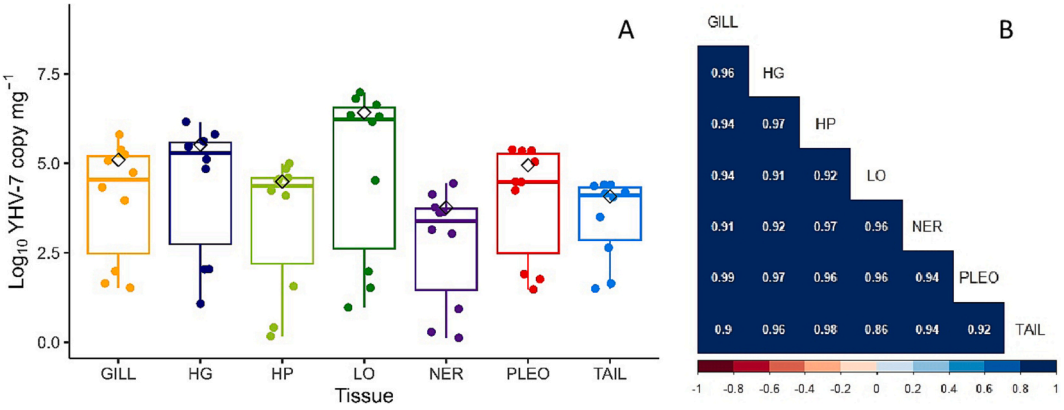

Fig. 4. (A) YHV-7 detection in different tissues of naturally infected *Penaeus monodon*. Each point represents the $\log_{10}$(YHV-7 copy number mg^{-1} tissue) calculated from the average cycle threshold value of technical triplicate RT-qPCR. No significant difference between means ($\alpha = 0.05$) were found. (B) Pearson's correlation coefficient matrix of $\log_{10}$(YHV-7 copy number mg^{-1} tissue) between tissue types. (GILL = gill, HG = hindgut, HP = hepatopancreas, LO = lymphoid organ, NER = ventral nerve cord, PLEO = pleopod, TAIL = tail muscle).

corroborative observation of Cowdry type A inclusion bodies and positive reaction by ISH, especially in *P. monodon* and *P. stylirostris*, or when infection loads are low (Aranguren Caro et al., 2022; Chayaburakul et al., 2005). As such, determining IHHNV infection status using histopathological observation of Cowdry type A inclusions or ISH may potentially yield false negative results. Therefore, molecular detection of IHHNV represents a more reliable means for determining IHHNV infection status.

There is growing evidence to substantiate the suitability of hepatopancreatic tissue as a target tissue for detection of IHHNV DNA using molecular techniques. For example, in naturally infected *P. monodon* similar infection levels were detected by PCR between hepatopancreas, heart, haematopoietic tissue, gill, subcutaneous tissue, pleopod, abdominal muscle, ventral nerve cord, lymphoid organ and haemolymph (Chayaburakul et al., 2005). Severe IHHNV infection of the hepatopancreas was detected by PCR in naturally infected *Macrobrachium rosenbergii,* with corroborating histology and ISH analysis (Hsieh et al., 2006). IHHNV DNA was also detected by PCR from hepatopancreas tissue in frozen commodity *Cherax quadricarinatus* (Lee et al., 2021). Most recently IHHNV was detected in hepatopancreas of experimentally challenged *Penaeus vannamei* by qPCR (Hou et al., 2023). In these studies, IHHNV was detected more reliably in hepatopancreas tissue, compared to other target tissues including gill (Lee et al., 2021), pleopod, and muscle tissue (Hou et al., 2023; Hsieh et al., 2006). In our study, detection of IHHNV from hepatopancreas yielded high copy number mg^{-1} tissue, with significant linear correlation to detection in other target tissues including the gill, lymphoid organ and pleopod. Our findings enhance the existing body of evidence, confirming that PCR-based detection of IHHNV from the hepatopancreas is possible and reliable. This evidence supports consideration for revision of current recommendations within the Aquatic Manual, specifically, that hepatopancreas be considered as a suitable tissue type for the detection of IHHNV.

Detection of IHHNV in the hindgut also yielded high IHHNV copy number mg^{-1} tissue, with significant linear correlation to detection in other target organs. This finding contrasts the Aquatic Manual's classification of enteric tissues as unsuitable for IHHNV surveillance and diagnostics. Nevertheless, our results suggest the potential suitability of this tissue, under the examined and specific conditions of this study. However, it is important to caution that commercial shrimp feeds frequently contain detectable template of shrimp pathogens (reviewed in Tacon, 2017). The potential for feed present in the gut of shrimp, containing non-viable pathogen template, to confound pathogen detection from hindgut samples should be considered. This study recognises the possible impact of this occurrence, especially since the timing between shrimp sampling and preceding feeding instances was not controlled. While this limitation is acknowledged, for all pathogen targets analysed, detection in the hindgut was significantly correlated with detection in other examined target organs. This strong correlation implies that any residual feed within the hindgut had minimal to no impact on the accurate detection of IHHNV, GAV, or YHV-7. Nonetheless, the potential for non-viable viral template in feed to erode the reliability of pathogen detection from the hindgut must be considered in result interpretation from this tissue.

The present study found IHHNV in the ventral nerve cord and tail muscle tissue to be significantly lower than other target organs, including gills. Chayaburakul et al. (2005) also found that the ventral nerve cord and muscle tissue of *P. monodon* were among the lowest ranking tissues for the detection of IHHNV, compared to eight other tissue types. Similarly, IHHNV detected in the tail muscle of *P. vannamei* in the study by Hou et al. (2023), yielded the lowest average copy number mg^{-1} tissue of all tissue types analysed. These findings together confer that muscle tissue and ventral nerve cord may be less suitable for reliable diagnostics and surveillance of IHHNV at lower viral loading, such as early in infection progression. The ventral nerve cord and ganglia are currently recommended as suitable target tissues for molecular detection of IHHNV within the Aquatic Manual (WOAH, 2023). Based on our analysis, and the additional works referenced, we suggest that sampling of nerve tissue is not advantageous for detection of IHHNV compared to other, more easily sampled tissue types such as gill or pleopod.

When considering non-destructive tissue sampling, gill and pleopod tissues are recommended for the detection of IHHNV (WOAH, 2023). Similar detection of IHHNV from pleopod and gill tissues was observed in a comparable study by Hou et al. (2023) in *P. vannamei*. In the present study, both gill and pleopod yielded high IHHNV copy number mg^{-1} tissue, were ranked among the best tissues, and detection between the two tissue types was highly correlated. This evidence suggests that gill or pleopod tissue would provide similar detection sensitivity for surveillance and diagnosis of IHHNV infection. Given the susceptibility of gill filaments to further damage during sampling (Mitchell et al., 2023), pleopod is likely preferential for non-lethal tissue sampling for IHHNV detection, despite gill tissue yielding negligibly increased copy number mg^{-1}.

4.2. YHV (Genotype 2 and 7)

Yellow head virus (YHV-1) has long been considered a significant pathogen of global shrimp aquaculture and was accordingly listed in the first edition of the Aquatic Code (OIE, 1995). While YHV-1 has never been reported from Australia, local variants of the yellow head complex including yellow head virus genotype 7 (YHV-7) and yellow head virus genotype 2, *syn* gill associated virus (GAV), are considered endemic within Australia.

Based on sequence analysis of ORF1b, the seventh distinct YHV genotype (YHV-7) shares highest similarity to YHV-1 (Mohr et al., 2015). YHV-7 was discovered in association with elevated mortalities among broodstock *P. monodon* originating from Northern Australia in 2012 (Mohr et al., 2015), and has since been detected in *P. monodon* sampled from various regions across Northern Australia between 2013 and 2019 (Arbon et al., 2022; Cowley et al., 2015, 2019). Pathogenicity of YHV-7 was demonstrated in *P. monodon* by experimental inoculation, resulting in cumulative mortality of approximately 60% at 28 days post-infection (Moody and Crane, 2016). YHV-7 outbreaks have also been associated with sporadic disease events in pond reared *P. monodon* (Cowley et al., 2019). As yet, YHV-7 has not been reported outside of Australia. Given the relatively modern discovery and its current containment to Australia, there are no known studies which investigate the tissue tropism of YHV-7. From the few studies published reporting the detection of YHV-7, detection has only been reported from pleopod, gill and epidermis tissues (Arbon et al., 2022; Cowley et al., 2019; Mohr, 2020; Mohr et al., 2015). Due to its apparent pathogenicity as indicated by both its association with mass mortality events on farm, and the experimental challenge conducted, current Australian shrimp aquaculture industry practice prioritises removal of broodstock with positive YHV-7 detection by RT-qPCR. As such, it is important to elucidate its tissue tropism for optimised detection by RT-qPCR.

YHV-7 and GAV are not listed in the Aquatic Code or Manual, therefore, no guidelines describing the selection of target tissues for their detection are available. However, given their relatedness to YHV-1 and current taxonomic classification within the same viral complex, the recommendations established for YHV-1 will be used as a proxy for YHV-7 and GAV (Mohr et al., 2015; Munro and Owens, 2007; Wijegoonawardane et al., 2009). These pathogens will herein be collectively referred to as yellow head viruses (YHV).

YHV is known to target tissues of the ectoderm and mesoderm (De La Vega et al., 2004; Munro and Owens, 2007; WOAH, 2023). While lymphoid organ is determined to be the primary target organ of YHV replication, the presence of YHV has been historically confirmed by bioassay, $TCID_{50}$ assay, Monoclonal Antibody, PCR, RT-qPCR, and classical histopathology in shrimp tissues including gill, gut, muscle, heart, nerve cord, hepatopancreas, haematopoietic tissue and

haemocytes, connective tissue, eyestalk and gonads, and hence YHV is considered a systemic virus (Chantanachookin et al., 1993; Cowley et al., 2002; Cowley et al., 2001; Lu et al., 1995; Soowannayan et al., 2002). To this body of evidence, we add the supporting results of the present study, which demonstrate non-significant differences in viral loading for both YHV genotypes (2 and 7) across pleopod, gill, lymphoid organ, hepatopancreas, hindgut, ventral nerve cord and abdominal muscle tissue.

While no significant differences in average copy number mg^{-1} tissue were detected, a clear advantage of lymphoid organ was observed for detection of YHV-7 and GAV, yielding the highest average copy number mg^{-1} tissue of the seven tissues analysed. Accordingly, this study supports the WOAH recommendation of lymphoid organ for detection of YHV (WOAH, 2023).

Given the systemic nature of YHV, currently, specific tissues that are unsuitable for the detection of YHV are not determined (WOAH, 2023). While detection of both YHV genotypes was statistically consistent among tissue types in the present study, there were clear disadvantages associated with sampling and analysis of ventral nerve cord and muscle tissues. This was especially evident for detection of GAV, where the overall range of detected GAV was lower, possibly reflective of sub-acute, chronic, or tolerated infection within the cohort. Based on GAV detection under these conditions, the results of the present study indicate that ventral nerve cord and tail muscle are least suitable for YHV detection as they may yield false negative results.

Gill and haemolymph are recommended as the most suitable samples for detection of YHV using non-destructive methods (WOAH, 2023). While detection of YHV genotypes 2 and 7 from haemolymph was not analysed in the present study, previous studies have strongly established its utility for reliable detection of YHV using RT-PCR and RT-qPCR (De La Vega et al., 2004; Kiatpathomchai et al., 2004; Ma et al., 2008). Detection of YHV genotypes 2 and 7 from gill tissue was analysed in the present study. Under the conditions of our analysis, consistent detection of GAV and YHV-7 between gill and pleopod tissues was observed, with strong correlation of detection within individual shrimps. Similar observations were made by Noble et al. (2018), where gill and pleopod tissues were demonstrated to yield similar GAV loading and variability from naturally infected *P. monodon*. As was apparent for the detection of IHHNV, this evidence suggests that gill or pleopod tissue would provide comparable detection sensitivity for surveillance and diagnosis of YHV infection.

4.3. Industry practices and implications

Based on the conditions analysed in the present study, lymphoid organ and hindgut consistently ranked among the best target tissues for IHHNV and YHV genotype 2 and 7. Targeting of lymphoid organ is recommended for the detection of IHHNV and YHV under surveillance conditions, when shrimp appear grossly normal (WOAH, 2023). Our findings support this strategy for the detection of YHV-7, YHV-2 (GAV), and IHHNV, when destructive sampling is permissible. The observed advantage of the lymphoid organ is likely related to its function in clearance of foreign material from the haemolymph (Rusaini, 2010). The involvement of the lymphoid organ in shrimp antiviral and antibacterial immunity potentiates it as a sensitive target tissue for detecting a range of pathogens, or their degraded products, in broader non-targeted screening and surveillance applications.

However, generally, the lymphoid organ in Penaeid shrimp is relatively small (1–4 mm in diameter), and its size and position within the shrimp cephalothorax can vary with shrimp species, sex, maturation stage, size, and health status (reviewed in Rusaini, 2010). Although there are advantages of sampling the lymphoid organ for detection sensitivity, sampling of the lymphoid organ can be challenging due to the small size and inconsistencies in its location within any given shrimp. Reliable collection of the lymphoid organ can become especially challenging when sampling is required from shrimp of a small size, shrimp which have been freeze-thawed, or when sampling is being conducted by untrained staff. Furthermore, for large-scale sampling, targeting such an organ becomes labour intensive and prone to error.

The findings of this study indicate that sampling of hindgut may permit a similar level of detection sensitivity to lymphoid organ for IHHNV and YHV. Given the difficulties of sampling the lymphoid organ, hindgut tissue may be a more practical target tissue for sampling. However, detection of any target from a hindgut sample must consider the presence of non-viable viral template in remnant feed within the hindgut (Tacon, 2017). Further work is required to elucidate the utility of the hindgut with respect to these factors, and throughout infection progression.

Detection from gills yielded the highest viral copy number of the non-destructive sample types assessed for all pathogen targets analysed. The highly correlated and comparable level of detection from pleopods and gills indicates that detection from pleopods will likely provide a similar level of detection sensitivity as gill tissue (Noble et al., 2018). Pleopods are already currently sampled from shrimp broadly across the shrimp aquaculture industry for routine pathogen screening (Arbon et al., 2022). Furthermore, sampling of gill tissue is more labour and skill intensive, and can frequently result in extensive damage to the sensitive gill structures (Mitchell et al., 2023). Continued use of pleopods for detection of IHHNV, as aligned with WOAH recommendations, and the addition of pleopods as a recommended target tissue for detection of YHV is expected to achieve comparable detection sensitivity while reducing the sampling burden on industry and potential damage to stock during sampling.

In addition to improving the detection of pathogens for surveillance and disease diagnosis, having an accurate understanding of virus distribution in shrimp tissues is an important consideration when devising risk management protocols to prevent the global transfer of shrimp pathogens within uncooked crustacean product (Lee et al., 2021). For example, Australia currently permits importation of uncooked shrimp product, given compliance of the imported product to specific conditions. The conditions permitting the import of uncooked shrimp product dictate the shrimp must be frozen, have head and shell removed, be deveined, and if not from a disease-free source, test free from WSSV and YHV-1 (DAFF, 2023).

While batch testing to confirm freedom of WSSV and YHV-1 provides adequate protection against importation of high risk material in most instances, this protection can be undermined by non-compliance with testing conditions by importers, weak border security assessment and inspection procedures, and variation in laboratory testing procedures and interpretation (Scott-Orr et al., 2017). In these cases, where testing cannot achieve reliable or complete protection, and for other pathogens beyond just WSSV and YHV-1, removal of the head, shell and hindgut from frozen shrimp is expected to reduce biosecurity risk to an appropriate level. In the present study, detection of the yellow head viruses was statistically similar from muscle tissue to other target tissues which are considered higher risk, including lymphoid organ, hepatopancreas and hindgut. These results indicate that current measures to de-risk importation of uncooked crustacean product into Australia, by removal of the head, shell, and deveining, may be inadequate to reduce exposure to yellow head virus, and other potential pathogens of consequence beyond those currently tested for (YHV-1 and WSSV) to confirm freedom. Further research is warranted to extend this evidence to pathogens of concern to national border security.

4.4. Considerations of experimental design

Biological and technical variability can produce differences in viral detection using qPCR across distinct tissue types. Biological variability relates to divergent virion concentration in different tissues due to complex host-pathogen interactions (referred to as tissue tropism). Technical variability stems from potential errors arising during sampling and analysis, such as procedural or human error, as well as the

technical capabilities and limitations of the technologies, including nucleic acid extraction platforms and protocols. To ensure the fidelity of this study's findings in reflecting biological variation of pathogen loading among tissues, various measures were taken to minimise the impact of potential technical variations on the analysis. Specifically, all sampling and analysis was conducted in compliance with international standard ISO/IEC 17025:2017 (ISO, 2017), and nucleic acid extraction and testing plans were designed to minimise potential inter-run or inter-batch reagent variation on subsequent tissue specific pathogen quantitation. Additionally, the potential for non-biological variability of viral quantification arising from the presence of PCR inhibitors within the different tissue samples was evaluated and considered.

Shrimp tissues including the compound eye and hepatopancreas are known to contain PCR inhibitors such as melanin-type compounds and polyphenols (Lin et al., 2022; Lo et al., 1997; Schrader et al., 2012; Wang et al., 1996), which may be co-extracted with target nucleic acid. Such inhibitors interfere with PCRs, preventing target amplification via interactions with the template, polymerase, or other reaction components (Buckwalter et al., 2014; Opel et al., 2010). Many modern commercial nucleic acid extraction and purification kits/protocols, including those employed in the present study, are increasingly robust against co-extraction of inhibitors and incorporate multiple measures to achieve this (e.g. use of solid-phase magnetic bead extraction (Bordelon et al., 2013), addition of a chaotropic agent such as guanidinium thiocyanate (Nelson and Krawetz, 1992), digestion with proteinase K (Rezadoost et al., 2016), and multiple staged wash phases (Jue et al., 2020)). The presence of PCR inhibitory compounds in shrimp tissues, including the hepatopancreas, has historically impacted the reliability of PCR analysis, and as such, these tissues are precluded from recommended diagnostic and surveillance samples types for certain WOAH listed diseases (Moody and Mohr, 2022; Richards, 1999; WOAH, 2023). However, for enteric diseases such as acute hepatopancreatic necrosis disease (AHPND) and infection with *Hepatobacter penaeii,* the Aquatic Manual recommends the targeted use of hepatopancreas for surveillance and diagnosis using qPCR (WOAH, 2023). While modern extraction chemistry and protocols are increasingly robust to the presence and impact of inhibitors, in these instances where recommended target tissues may contain inhibitors, the inclusion of an internal process control (e.g. qPCR assay targeting a shrimp house-keeping gene) is required to demonstrate that the nucleic acid extracted from these tissues is free from inhibitors (Moody and Mohr, 2022; Schrader et al., 2012). In the present study, the *P. monodon* Dicer-1 gene (*syn* Pm Dcr1) was used as an internal control. Dicer-1, involved in the crustacean RNA interference pathway, was selected due to its systemic and independent expression from viral genetic loads in shrimp naturally infected with GAV (Su et al., 2008). Within all examined tissue types, no significant, or notable non-significant negative correlations were observed between the detection levels of the Dicer-1 and the quantity of tissue used in nucleic acid extraction and purification. This measure, indicative of the potential presence of co-precipitated inhibitors, demonstrates either the absence of inhibitors in the purified template or the robustness of subsequent qPCR analysis to their influence. In either case, the absence of a discernible effect supports the robustness of the results and attribution of the variability observed in pathogen detection between tissue types to biological causes, including viral tissue tropism and host-pathogen interactions.

While multiple measures were incorporated to ensure the fidelity of its results with respect to the detection of real biological variation of viral loading between tissues, there are two notable limitations of our study. Firstly, while the detections of each pathogen target were diverse (IHHNV: $\sim 10^4$–10^8, YHV-7: <10–10^6, GAV: undetectable – 10^6 copies mg^{-1} tissue), all shrimp analysed were naturally infected, and were collected from a single production pond at a single timepoint. Consequently, infection progression was not controlled for, or able to be measured. Diagnostic sensitivity from specific tissues may be reduced at lower infection severity, or early in the progress of infection (Chayaburakul et al., 2005; Kim et al., 2023). As such, further analysis may be required to elucidate the qPCR detection patterns observed in the present study at different stages of infection.

The multiple measures conducted to ensure the fidelity of the results, could also be considered as a limiting factor for this study. While the nucleic acid extraction platform (MagMAX™ CORE Nucleic Acid Purification Kit with KingFisher™ Flex 96 Deep-Well Magnetic Particle Processor), qPCR assays (Cowley et al., 2019; Cowley et al., 2018; De La Vega et al., 2004; Su et al., 2008), qPCR master mix (SensiFAST™ Probe Lo-ROx Kit and SensiFAST™ Probe Lo-ROx One-Step Kit) and instrument (QuantStudio™ 5 Real-Time PCR System, 384-well) utilised in this study were selected to yield highly reliable detection, robust to the presence of PCR inhibitors, we recognise that these conditions are not widely attainable. Consequently, it is acknowledged that factors including the presence of inhibitory compounds in shrimp tissues presents ongoing challenges for diagnosis and surveillance of shrimp pathogens when such conditions have not yet been adopted or are not readily available. Extension of these studies to incorporate analysis of detection results from tissues extracted and tested using other platforms and commercially available kits is needed (Buckwalter et al., 2014). Irrespective of the availability of such evidence, it remains essential to consistently implement internal process controls within analysis.

4.5. Conclusions

Definition and recommendation of the appropriate target tissue is crucial to enable accurate pathogen detection in both diagnostic and surveillance applications to shrimp aquaculture using real-time PCR analysis. This study reports tissue-specific qPCR detection of genetic viral loads in pleopod, gill, hepatopancreas, lymphoid organ, abdominal muscle tissue, hindgut and ventral nerve cord from *P. monodon* naturally infected with IHHNV, YHV-2/GAV or YHV-7. The results presented confirm detection of high load IHHNV from hepatopancreas tissue, and highlight pleopod tissue as a comparably sensitive alternative tissue to gills for the detection of YHV. These findings indicate that current recommendations for target tissues of IHHNV and YHV provided in the WOAH Aquatic Manual may require revision, however, we underline the need for extension of similar research to support broader review and modification of the Aquatic Manual. The results of this study will be valuable for understanding infection patterns of IHHNV and YHV, not only to improve their detection for surveillance and disease diagnosis, but also for consideration when devising risk management protocols to prevent the global transfer of shrimp pathogens within uncooked crustacean product.

CRediT authorship contribution statement

P.M. Arbon: Conceptualization, Data curation, Formal analysis, Investigation, Visualization, Writing – original draft, Writing – review & editing. **M. Andrade Martinez:** Investigation, Writing – review & editing. **M. Garrett:** Investigation. **D.R. Jerry:** Writing – review & editing. **K. Condon:** Conceptualization, Funding acquisition, Resources, Writing – review & editing.

Declaration of competing interest

The authors declare that they have no known competing financial interests or personal relationships that could have appeared to influence the work reported in this paper.

Data availability

The data that support the findings of this study are available from the corresponding author upon reasonable request.

Acknowledgements

Phoebe Arbon was supported through an Australian Government Research Training Program (RTP) scholarship through James Cook University (JCU) and the Cooperative Research Centre for Developing Northern Australia (CRCNA; Project No. A32021044). This research was funded by the CRCNA Project No. A32021044, and is supported by the Cooperative Research Centres Program, an Australian Government Initiative. The CRCNA also acknowledges the support of its investment partners: the Western Australian, Northern Territory and Queensland Governments. This CRCNA project was supported by the Australian Prawn Farmers Association (APFA) and the Fisheries Research and Development Corporation (FRDC). The authors acknowledge the in-kind support of the APFA, APFA members and JCU.

References

Aranguren Caro, L.F., Gomez-Sanchez, M.M., Piedrahita, Y., Mai, H.N., Cruz-Flores, R., Alenton, R.R.R., Dhar, A.K., 2022. Current status of infection with infectious hypodermal and hematopoietic necrosis virus (IHHNV) in the Peruvian and Ecuadorian shrimp industry. PLoS One 17, e0272456. https://doi.org/10.1371/journal.pone.0272456.

Arbon, P.M., Condon, K., Andrade Martinez, M., Jerry, D.R., 2022. Molecular detection of six viral pathogens from Australian wild sourced giant black tiger shrimp (Penaeus monodon) broodstock. Aquaculture 548, 737651. https://doi.org/10.1016/j.aquaculture.2021.737651.

Asche, F., Anderson, J.L., Botta, R., Kumar, G., Abrahamsen, E.B., Nguyen, L.T., Valderrama, D., 2021. The economics of shrimp disease. J. Invertebr. Pathol. 186, 107397 https://doi.org/10.1016/j.jip.2020.107397.

Bordelon, H., Russ, P.K., Wright, D.W., Haselton, F.R., 2013. A magnetic bead-based method for concentrating DNA from human urine for downstream detection. PLoS One 8, e68369. https://doi.org/10.1371/journal.pone.0068369.

Buckwalter, S.P., Sloan, L.M., Cunningham, S.A., Espy, M.J., Uhl, J.R., Jones, M.F., Vetter, E.A., Mandrekar, J., Cockerill, F.R., Pritt, B.S., Patel, R., Wengenack, N.L., 2014. Inhibition controls for qualitative real-time PCR assays: are they necessary for all specimen matrices? J. Clin. Microbiol. 52, 2139–2143. https://doi.org/10.1128/JCM.03389-13.

Chantanachookin, C., Boonyaratpalin, S., Kasornchandra, J., Direkbusarakom, S., Ekpanithanpong, U., Supamataya, K., Sriurairatana, S., Flegel, T., 1993. Histology and ultrastructure reveal a new granulosis-like virus in Penaeus monodon affected by yellow-head disease. Dis. Aquat. Org. 17, 145–157. https://doi.org/10.3354/dao017145.

Chayaburakul, K., Lightner, D.V., Sriurairattana, S., Nelson, K.T., Withyachumnarnkul, B., 2005. Different responses to infectious hypodermal and hematopoietic necrosis virus (IHHNV) in Penaeus monodon and P. Vannamei. Dis. Aquat. Org. 67, 191–200. https://doi.org/10.3354/dao067191.

Cowley, J.A., Dimmock, C.M., Spann, K.M., Walker, P.J., 2001. Gill-Associated Virus of Penaeus Monodon Prawns. Springer, Boston, MA, pp. 43–48. https://doi.org/10.1007/978-1-4615-1325-4_6.

Cowley, J.A., Hall, M.R., Cadogan, L.C., Spann, K.M., Walker, P.J., 2002. Vertical transmission of gill-associated virus (GAV) in the black tiger prawn Penaeus monodon. Dis. Aquat. Org. 50, 95–104. https://doi.org/10.3354/dao050095.

Cowley, J., Moody, N.J.G., Mohr, P.G., Rao, M., Cowley, J., 2015. Tactical Research Fund : Aquatic Animal Health Subprogram : Viral presence, prevalence and disease management in wild populations of the Australian Black Tiger prawn (Penaeus monodon) Lynette M Williams, Melony J Sellars, Mark StJ Crane June 2015 FRD. FRDC.

Cowley, J.A., Rao, M., Coman, G.J., 2018. Real-time PCR tests to specifically detect IHHNV lineages and an IHHNV EVE integrated in the genome of Penaeus monodon. Dis. Aquat. Org. 129, 145–158. https://doi.org/10.3354/dao03243.

Cowley, J.A., Rao, M., Mohr, P., Moody, N.J., Sellars, M.J., Crane, M.S., 2019. TaqMan real-time and conventional nested PCR tests specific to yellow head virus genotype 7 (YHV7) identified in giant tiger shrimp in Australia. J. Virol. Methods 273, 113689. https://doi.org/10.1016/j.jviromet.2019.113689.

DAFF, 2023. Review of the Biosecurity Risks of Prawns Imported from all Countries for Human Consumption - Final Report. Canberra, Australia.

De La Vega, E., Degnan, B.M., Hall, M.R., Cowley, J.A., Wilson, K.J., 2004. Quantitative real-time RT-PCR demonstrates that handling stress can lead to rapid increases of gill-associated virus (GAV) infection levels in Penaeus monodon. Dis. Aquat. Org. 59, 195–203. https://doi.org/10.3354/dao059195.

Fox, J., Weisberg, S., 2019. An R Companion to Applied Regression, Third. ed. Sage, Thousand Oaks CA.

Harrell, F.E., 2023. Package "Hmisc" title Harrell miscellaneous. In: Comprehensive R Archive Network (CRAN).

Hou, Z.H., Gao, Y., Wang, J.J., Chen, C.Y., Chang, L.R., Li, T., Si, L.J., Li, F., Yan, D.C., 2023. Study of infectious hypodermal and hematopoietic necrosis virus (IHHNV) infection in different organs of Penaeus vannamei. J. Invertebr. Pathol. 199, 107952 https://doi.org/10.1016/J.JIP.2023.107952.

Hsieh, C.Y., Chuang, P.C., Chen, L.C., Chien, Tu, Chien, M.S., Huang, K.C., Kao, H.F., Tung, M.C., Tsai, S.S., 2006. Infectious hypodermal and haematopoietic necrosis virus (IHHNV) infections in giant freshwater prawn, Macrobrachium rosenbergii. Aquaculture 258, 73–79. https://doi.org/10.1016/J.AQUACULTURE.2006.04.007.

ICTV, 2023. The ICTV Report on Virus Classification and Taxon Nomenclature: Genus Penstyldensovirus.

ISO, 2017. ISO/IEC 17025 - General Requirements for the Competence of Testing and Calibration Laboratories, 1st ed. International Organization for Standardization, Geneva, Switzerland.

Jue, E., Witters, D., Ismagilov, R.F., 2020. Two-phase wash to solve the ubiquitous contaminant-carryover problem in commercial nucleic-acid extraction kits. Sci. Rep. 10, 1940. https://doi.org/10.1038/s41598-020-58586-3.

Kennedy, D.A., Kurath, G., Brito, I.L., Purcell, M.K., Read, A.F., Winton, J.R., Wargo, A. R., 2016. Potential drivers of virulence evolution in aquaculture. Evol. Appl. 9, 344–354. https://doi.org/10.1111/EVA.12342.

Kiatpathomchai, W., Jitrapakdee, S., Panyim, S., Boonsaeng, V., 2004. RT-PCR detection of yellow head virus (YHV) infection in Penaeus monodon using dried haemolymph spots. J. Virol. Methods 119, 1–5. https://doi.org/10.1016/j.jviromet.2004.02.008.

Kim, M.-J., Kim, J.-O., Jang, G.-I., Kwon, M.-G., Kim, K.-I., 2023. Diagnostic validity of molecular diagnostic assays for white spot syndrome virus at different severity grades. Heliyon 9, e19351. https://doi.org/10.1016/j.heliyon.2023.e19351.

Kumar, V., Roy, S., Behera, B.K., Das, B.K., 2022. Disease diagnostic tools for health Management in Aquaculture. In: Advances in Fisheries Biotechnology. Springer Nature, pp. 363–382. https://doi.org/10.1007/978-981-16-3215-0_21.

Lee, C., Choi, S.-K., Jeon, H.J., Lee, S.H., Kim, Y.K., Park, S., Park, J.-K., Han, S.-H., Bae, S., Kim, J.H., Han, J.E., 2021. Detection of infectious hypodermal and hematopoietic necrosis virus (IHHNV, decapod Penstylhamaparvovirus 1) in commodity red claw crayfish (Cherax quadricarinatus) imported into South Korea. J. Mar. Sci. Eng. 9, 856. https://doi.org/10.3390/jmse9080856.

Leung, T.L.F., Bates, A.E., 2013. More rapid and severe disease outbreaks for aquaculture at the tropics: implications for food security. J. Appl. Ecol. 50, 215–222. https://doi.org/10.1111/1365-2644.12017.

Lightner, D.V., 1993. Diseases of Penaeid shrimp. In: Press, C.R.C. (Ed.), CRC Handbook of Mariculture: Crustacean Aquaculture, 1. Boca Raton, Florida, USA, pp. 389–402.

Lightner, D.V., Redman, R.M., 1998. Shrimp diseases and current diagnostic methods. In: Aquaculture. Elsevier, pp. 201–220. https://doi.org/10.1016/S0044-8486(98)00187-2.

Lightner, D.V., Redman, R.M., Bell, T.A., 1983. Infectious hypodermal and hematopoietic necrosis, a newly recognized virus disease of penaeid shrimp. J. Invertebr. Pathol. 42, 62–70. https://doi.org/10.1016/0022-2011(83)90202-1.

Lightner, D.V., Redman, R.M., Bell, T.A., Brock, J.A., 2009. Detection of IHHN virus in Penaeus stylirostris AND P. vannamei imported into Hawaii. J. World Maric. Soc. 14, 212–225. https://doi.org/10.1111/j.1749-7345.1983.tb00077.x.

Lin, H.Y., Yen, S.C., Tsai, S.K., Shen, F., Lin, J.H.Y., Lin, H.J., 2022. Combining direct PCR technology and capillary electrophoresis for an easy-to-operate and highly sensitive infectious disease detection system for shrimp. Life 12. https://doi.org/10.3390/life12020276.

Lo, C.F., Ho, C.H., Chen, C.H., Liu, K.F., Chiu, Y.L., Yeh, P.Y., Peng, S.E., Hsu, H.C., Liu, H.C., Chang, C.F., Su, M. Sen, Wang, C.H., Kou, G.H., 1997. Detection and tissue tropism of white spot syndrome baculovirus (WSBV) in captured brooders of Penaeus monodon with a special emphasis on reproductive organs. Dis. Aquat. Org. 30, 53–72. https://doi.org/10.3354/dao030053.

Lu, Y., Tapay, L., Loh, P., Brock, J., Gose, R., 1995. Distribution of yellow-head virus in selected tissues and organs of penaeid shrimp Penaeus vannamei. Dis. Aquat. Org. 23, 67–70. https://doi.org/10.3354/dao023067.

Ma, H., Overstreet, R.M., Jovonovich, J.A., 2008. Stable yellowhead virus (YHV) RNA detection by qRT-PCR during six-day storage. Aquaculture 278, 10–13. https://doi.org/10.1016/j.aquaculture.2008.03.028.

Mitchell, S.O., Scholz, F., Marcos, M., Rodger, H., 2023. Sampling artefacts in gill histology of freshwater Atlantic salmon (*Salmo salar*). Bull. Eur. Assoc. Fish Pathol. 43, 1–11. https://doi.org/10.48045/001C.68302.

Mohr, P., 2020. Detection and pathogenicity of yellow head virus genotypes one and seven. In: 11th Annual Workshop of the National Reference Laboratories for Crustacean Diseases, Technical University of Denmark, Lyngby, 4-5th November 2020. EURL fish and crustacean diseases. csiro:EP207655, p. 1.

Mohr, P., Moody, N., Hoad, J., Williams, L., Bowater, R., Cummins, D., Cowley, J., Crane, M.S., 2015. New yellow head virus genotype (YHV7) in giant tiger shrimp Penaeus monodon indigenous to northern Australia. Dis. Aquat. Org. 115, 263–268. https://doi.org/10.3354/dao02894.

Moody, N.J.G., Crane, M., 2016. FRDC 2015-015: Aquatic Animal Health Subprogram: Determining the Susceptibility of Australian Penaeus Monodon and P. Merguiensis to Newly Identified Enzootic (YHV7) and Exotic (YHV8 and YHV10) Yellow Head Virus (YHV) Genotypes.

Moody, N., Mohr, P., 2022. Australian and New Zealand Standard Diagnostic Procedure (ANZSDP) for White Spot Syndrome Virus 7–12.

Munro, J., Owens, L., 2007. Yellow head-like viruses affecting the penaeid aquaculture industry: a review. Aquac. Res. 38, 893–908. https://doi.org/10.1111/j.1365-2109.2007.01735.x.

Nelson, J.E., Krawetz, S.A., 1992. Purification of cloned and genomic DNA by guanidine thiocyanate/isobutyl alcohol fractionation. Anal. Biochem. 207, 197–201. https://doi.org/10.1016/0003-2697(92)90523-A.

Noble, T.H., Stratford, C.N., Wade, N.M., Cowley, J.A., Sellars, M.J., Coman, G.J., Jerry, D.R., 2018. PCR testing of single tissue samples can result in misleading data on gill-associated virus infection loads in shrimp. Aquaculture 492, 91–96. https://doi.org/10.1016/j.aquaculture.2018.03.028.

Ogle, D., Doll, J.C., Powell Wheeler, A., Dinno, A., 2022. Simple Fisheries Stock Assessment Methods (FSA) v 0.9.3.

OIE, 1995. International Aquatic Animal Health Code, 1st ed. Office International des Epizooties, World Organisation for Animal Health, Paris, France.
OIE, 2019. Manual of Diagnostic Tests for Aquatic Animals: Chapter 2.2.4. Infection with Infectious Hypodermal and Haematopoietic Necrosis Virus.
Opel, K.L., Chung, D., McCord, B.R., 2010. A study of PCR inhibition mechanisms using real time PCR*,†. J. Forensic Sci. 55, 25–33. https://doi.org/10.1111/J.1556-4029.2009.01245.X.
Pulkkinen, K., Suomalainen, L.R., Read, A.F., Ebert, D., Rintamäki, P., Valtonen, E.T., 2010. Intensive fish farming and the evolution of pathogen virulence: the case of columnaris disease in Finland. Proc. R. Soc. B Biol. Sci. 277, 593. https://doi.org/10.1098/RSPB.2009.1659.
R Core Team, 2022. R: A Language and Environment for Statistical Computing. R Foundation for Statistical Computing.
Rezadoost, M.H., Kordrostami, M., Kumleh, H.H., 2016. An efficient protocol for isolation of inhibitor-free nucleic acids even from recalcitrant plants. 3 Biotech 6, 1–7. https://doi.org/10.1007/S13205-016-0375-0.
Richards, G.P., 1999. Limitations of molecular biological techniques for assessing the virological safety of foods. J. Food Prot. 62, 691–697. https://doi.org/10.4315/0362-028X-62.6.691.
Rusaini, Owens L., 2010. Insight into the lymphoid organ of penaeid prawns: a review. Fish Shellfish Immunol. 29, 367–377. https://doi.org/10.1016/J.FSI.2010.05.011.
Schrader, C., Schielke, A., Ellerbroek, L., Johne, R., 2012. PCR inhibitors - occurrence, properties and removal. J. Appl. Microbiol. 113, 1014–1026. https://doi.org/10.1111/j.1365-2672.2012.05384.x.
Scott-Orr, H., Jones, B., Bhatia, N., 2017. Uncooked Prawn Imports:Effectiveness of Biosecurity Controls. Australian Government, Inspector-General of Biosecurity, p. 2017.
Shinn, A.P., Pratoomyot, J., Griffiths, D., Trong, T.Q., Vu, N.T., Jiravanichpaisal, P., Briggs, M., 2018. Asian shrimp production and the economic costs of disease. Asian Fish. Sci. 31S, 29–58. https://doi.org/10.33997/j.afs.2018.31.S1.003.
Soowannayan, C., Sithigorngul, P., Flegel, T.W., 2002. Use of a specific monoclonal antibody of determine tissue tropism of yellow head virus (YHV) of Penaeus monodon by in situ immunocytochemistry. Fish. Sci. 68, 805–809. https://doi.org/10.2331/fishsci.68.sup1_805.
Stentiford, G.D., Neil, D.M., Peeler, E.J., Shields, J.D., Small, H.J., Flegel, T.W., Vlak, J. M., Jones, B., Morado, F., Moss, S., Lotz, J., Bartholomay, L., Behringer, D.C., Hauton, C., Lightner, D.V., 2012. Disease will limit future food supply from the global crustacean fishery and aquaculture sectors. J. Invertebr. Pathol. https://doi.org/10.1016/j.jip.2012.03.013.
Stentiford, G.D., Sritunyalucksana, K., Flegel, T.W., Williams, B.A.P., Withyachumnarnkul, B., Itsathitphaisarn, O., Bass, D., 2017. New paradigms to help solve the global aquaculture disease crisis. PLoS Pathog. 13, e1006160 https://doi.org/10.1371/journal.ppat.1006160.
Su, J., Oanh, D.T.H., Lyons, R.E., Leeton, L., van Hulten, M.C.W., Tan, S.-H., Song, L., Rajendran, K.V., Walker, P.J., 2008. A key gene of the RNA interference pathway in the black tiger shrimp, Penaeus monodon: identification and functional characterisation of Dicer-1. Fish Shellfish Immunol. 24, 223–233. https://doi.org/10.1016/j.fsi.2007.11.006.
Tacon, A.G.J., 2017. Biosecure shrimp feeds and feeding practices: guidelines for future development. J. World Aquacult. Soc. 48, 381–392. https://doi.org/10.1111/jwas.12406.
Valappil, R.K., Stentiford, G.D., Bass, D., 2021. The rise of the syndrome – sub-optimal growth disorders in farmed shrimp. Rev. Aquac. 13, 1888–1906. https://doi.org/10.1111/raq.12550.
Walker, P.J., Winton, J.R., 2010. Emerging viral diseases of fish and shrimp. Vet. Res. 41, 51. https://doi.org/10.1051/VETRES/2010022.
Wang, S.Y., Hong, C., Lotz, J.M., 1996. Development of a PCR procedure for the detection of Baculovirus penaei in shrimp. Dis. Aquat. Org. 25, 123–131. https://doi.org/10.3354/dao025123.
Wijegoonawardane, P.K.M., Sittidilokratna, N., Petchampai, N., Cowley, J.A., Gudkovs, N., Walker, P.J., 2009. Homologous genetic recombination in the yellow head complex of nidoviruses infecting Penaeus monodon shrimp. Virology 390, 79–88. https://doi.org/10.1016/j.virol.2009.04.015.
WOAH, 2023. Manual of Diagnostic Tests for Aquatic Animals, 10th ed. World Organisation for Animal Health.